IJECEC INTERNATIONAL JOURNAL OF ELECTRICAL AND COMPUTER COMMUNICATION ENGINEERING
ISSN (Online):2533-8945
VOLUME 3 ISSUE 2

DYNAMIC PHASOR-BASED SIMULATION OF UNBALANCED RADIAL DISTRIBUTION SYSTEMS OF PV SYSTEM

B.SHIVA PRASANNA, PG STUDENT

K.SABITHA, ASSISTANT PROFESSOR

K.V.SUBBAREDDY COLLEGE OF ENGINEERING FOR WOMEN, KURNOOL

Abstract— This paper develops an analytical model of an unbalanced radial distribution system consisting of a single-phase photovoltaic (PV), a three-phase induction machine load, a three-phase power factor correction capacitor (PFC), and a load. The analytical model is based on dynamic phasors (DP) for phases. The single-phase PV model includes inverter current control [proportional resonance (PR) controller], an L, or an LCL filter. The induction machine model is based on positive-, negative-, and zerosequence components' dynamic phasors. The sequence-based induction machine model was converted to the DP- reference frame and interconnected with other grid components. The developed analytical model is capable of small-signal analysis and can be used to identify variety of stability and/or harmonic issues in distribution networks, e.g., instability due to weak grid. Impact of unbalance on system dynamic performance can also be investigated using this model. The analytical model is benchmarked with a high-fidelity model built in Matlab/SimPowerSystems where power electronic switching details are included. The small-signal analysis results are validated via Matlab/SimPowerSystems timedomain simulations.

Index Terms— Dynamic phasor (DP), induction machine, singlephase photovoltaic, small-signal analysis.

I. INTRODUCTION

INCREASING efficiency and decreasing cost of solar technology promotes substantial growth of photovoltaic (PV) power integration in modern power systems. The total capacity of grid connected PV systems has increased from 300 MW in 2000 to 21 GW in 2010 [1]. PV has shared a fair amount of renewable energy penetration in microgrids where the PV power supplies electrical loads for local communities [2]–[4]. New government policies and incentives encourage more and more single-phase PV systems to be connected. In addition, induction machine-based loads are dominant in distribution systems. Analytical models of such unbalanced distribution systems would provide insights of the system and further be used for smallsignal and large-signal stability analysis.

The analysis will help identify stability issues and mitigate related problems. For unbalanced systems, frame-based dynamic models can be used for dynamic performance examination. Simulation packages such as Matlab/SimPowerSystems [6] are based on simulation models with instantaneous variables, e.g., instantaneous voltages and currents in three phases. Conventional linearization at an operating condition cannot be applied to these models due to the periodic varying state variables. The necessary condition for small-signal analysis is to have constant values for state variables at steady state [7]. Transforming the models to a synchronous rotating reference frame is the most common technique utilized to overcome the above problem [7]. However the negative-sequence components presented in an unbalance system will be converted to 120-Hz ac variables in a -reference frame. Hence, -reference framebased models do not offer the capability of small-signal analysis under unbalanced topology and operating conditions.

On the other hand, dynamic phasor (DP)-based modeling, an averaging technique, has been demonstrated to be capable of converting periodic varying state variables into dc state variables. It has been used in electrical machines analysis [8], [9], dc/dc converter analysis, distribution system analysis, and HVDC and FACTS system modeling and analysis. For example, presents an averaged model of LCC-based HVDC system which is capable of representing low frequency dynamics of the converters at both AC and DC sides. DP models make small-signal analysis feasible. Small-signal analysis based on DP models has been carried out . DP modeling technique also provides very accurate simulations for larger time steps .

Moreover, DP-based modeling can take into consideration of unbalance. For example, in [9], an induction machine (IM) model as well as a permanent magnet synchronous generator (PMSG) model in unbalanced conditions have been developed

ISSN (Online):2533-8945
VOLUME 3 ISSUE 2

based on positive, negative, and zero (pnz) variables. In [11], the dynamic phasor-based modeling technique is used to model the unified power flow controller (UPFC). The model is expressed in pnz variables and can be used to study the effect of unbalanced operation. [16] presents a DP-based model taking into consideration of positive-, negative, and zero-sequence elements of a synchronous generator and its voltage controls. Tests on a single-machine infinite-bus system is conducted

The above-mentioned references [9], consider only unbalanced operation instead of unbalanced topology. The objective of this paper is to model, analyze and simulate an unbalanced distribution system with both complex loads such as IM and renewables such as inverter interfaced PVs. To the authors' best knowledge, the literature lacks a comprehensive modeling approach for unbalanced distribution systems that is suitable for both small-signal analysis and nonlinear time-domain simulation.

An effort has been taken in [7] to model a distribution system with unbalanced topology. The system model is expressed by DPs of fundamental frequency in frame and the system contains a synchronous generator and a single-phase inverter. Our proposed work will improve the modeling strategy in two aspects and therefore tackle comprehensive dynamic phenomena of unbalanced distribution systems.

• A more comprehensive inverter control will be modeled in this paper. The inverter is modeled in [7] as a PQ controlled voltage source. Current controls are ignored. Interactions between the current controls of inverters and the grid can lead to resonances [18]. Therefore, ignoring current controls of a grid-connected inverter will lead to the omission of certain dynamics. The current controls of a PV inverter will be modeled in our paper.

• A more comprehensive system model will be pursued in this paper. The network model is treated as algebraic equations with dynamics of inductors and capacitors ignored. Each source in the system is treated as a voltage source. The sources are interfaced through voltage/ current algebraic relationship derived based on the network model. In our paper, a different modeling strategy is adopted. Each source is modeled as a current source. The sources are then interfaced through network dynamics. Using this strategy, the network dynamics due to inductors and capacitors will not be omitted. In summary, this paper investigates comprehensive modeling of unbalanced distribution systems using dynamic phasors.

The system consists of a three-phase induction machine load, threephase resistive loads, a PFC and a single-phase PV system. The three-phase induction machine, will be modeled based on dynamic phasors and then be converted to phasors. A single-phase PV system at phase will be modeled in phase phasors. The entire system model will be obtained through a current source-based integration technique. The major contributions of this paper include a comprehensive dynamic modeling approach for unbalanced radial distribution systems. Applications of the model will be demonstrated in small-signal analysis and fast and accurate simulation. Though the study system has only one single-phase source, the proposed modeling method can be applied to radial systems with multiple unbalanced components. The easiness of integrating multiple unbalanced elements will be shown.

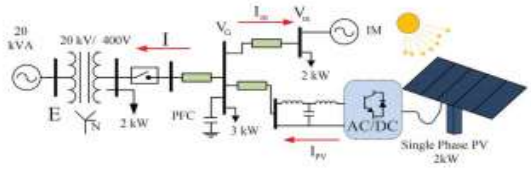

Fig. 1. Study system.

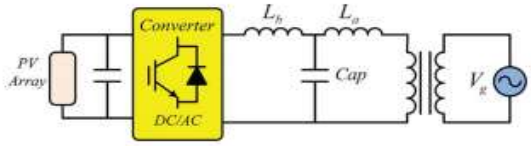

Fig. 2. Basic configuration of PV system.

II.PHOTOVOLTAIC INVERTER

The basic block diagram of grid connected PV power generation system is shown in Fig. 2.1.
The PV power generation system consists of following major blocks:

1. PV unit
2. Inverter
3. Grid
4. MPPT

ISSN (Online):2533-8945
VOLUME 3 ISSUE 2

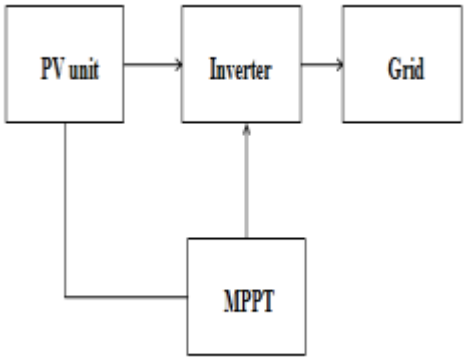

Fig. 3 Schematic diagram of PV system

1. PV unit : A PV unit consists of number of PV cells that converts the energy of light directly into electricity (DC) using photovoltaic effect.
2. Inverter : Inverter is used to convert DC output of PV unit to AC power.
3. Grid : The output power of inverter is given to the nearby electrical grid for the power generation.
4. MPPT : In order to utilize the maximum power produced by the PV modules, the power conversion equipment has to be equipped with a maximum power point tracker (MPPT). It is a device which tracks the voltage at where the maximum power is utilized at all times.

For the design of PV generation system, the specifications of considered PV system are shown in below Table 2.1

2.1.1 Photovoltaic Cell and Array Modeling

A PV cell is a simple p-n junction diode that converts the irradiation into electricity. Fig.3.1 illustrates a simple equivalent circuit diagram of a PV cell. This model consists of a current source which represents the generated current from PV cell, a diode in parallel with the current source, a shunt resistance, and a series resistance.

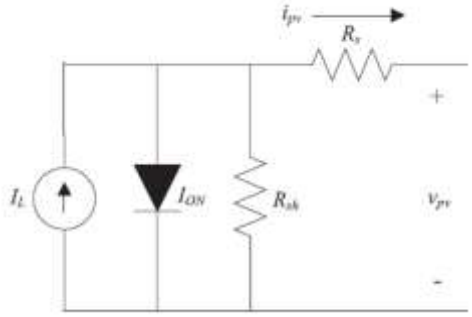

Fig.4 Equivalent circuit diagram of the PV cell

III.DC-DC Converter Basics

A DC-to-DC converter is a gadget that acknowledges a DC info voltage and produces a DC yield voltage. Normally the yield delivered is at an alternate voltage level than the info. Also, DC-to-DC converters are utilized to give clamor confinement, force transport regulation, and so on. This is a synopsis of a portion of the prevalent DC-to-DC converter topologies.

3.1 BUCK CONVERTER

In this circuit the transistor turning ON will put voltage Vin toward one side of the inductor. This voltage will tend to bring about the inductor current to rise. At the point when the transistor is OFF, the present will keep coursing through the inductor however now moving through the diode.

We at first accept that the current through the inductor does not achieve zero, in this way the voltage at Vx will now be just the voltage over the leading diode amid the full OFF time. The normal voltage at Vx will rely on upon the normal ON time of the transistor gave the inductor current is persistent.

ISSN (Online):2533-8945
VOLUME 3 ISSUE 2

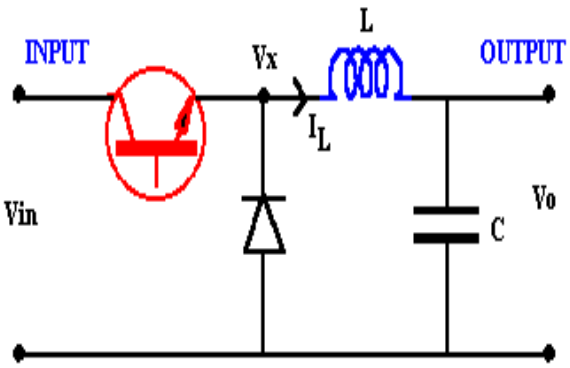

Fig 5 Buck Converter

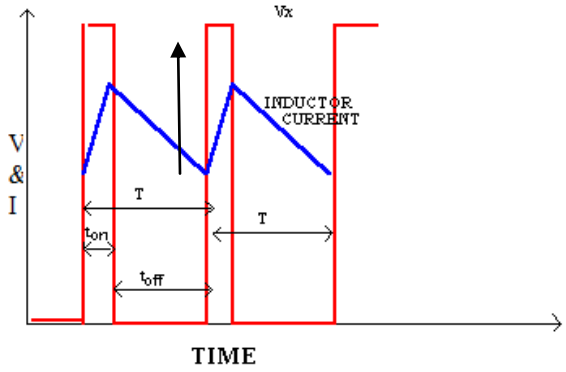

Fig6: Voltage and current changes

IV.INDUCTION MOTOR

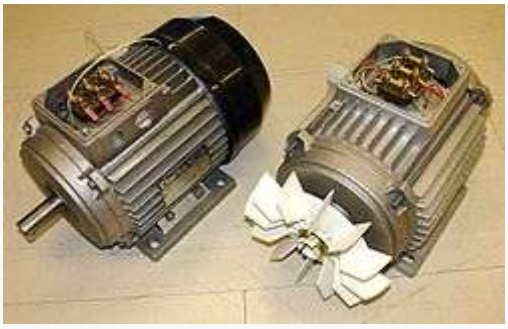

Three-phase totally enclosed fan-cooled (TEFC) induction motor with end cover on the left, and without end cover to show cooling fan. In TEFC motors, interior losses are dissipated indirectly through enclosure fins mostly by forced air convection.

An **asynchronous motor** type of an **induction motor** is an AC electric motor in which the electric current in the rotor needed to produce torque is obtained by electromagnetic induction from the magnetic field of the stator winding. An induction motor can therefore be made without electrical connections to the rotor as are found in universal, DC and synchronous motors. An asynchronous motor's rotor can be either wound type or squirrel-cage type.

Three-phase squirrel-cage asynchronous motors are widely used in industrial drives because they are rugged, reliable and economical. Single-phase induction motors are used extensively for smaller loads, such as household appliances like fans. Although traditionally used in fixed-speed service, induction motors are increasingly being used with variable-frequency drives (VFDs) in variable-speed service. VFDs offer especially important energy savings opportunities for existing and prospective induction motors in variable-torque centrifugal fan, pump and compressor load applications. Squirrel cage induction motors are very widely used in both fixed-speed and variable-frequency drive (VFD) applications. Variable voltage and variable frequency drives are also used in variable-speed service.

4.1 Principles of operation:

In both induction and synchronous motors, the AC power supplied to the motor's stator creates amagnetic field that rotates in time with the AC oscillations. Whereas a synchronous motor's rotor turns at the same rate as the stator field, an induction motor's rotor rotates at a slower speed than the stator field. The induction motor stator's magnetic field is therefore changing or rotating relative to the rotor. This induces an opposing current in the induction motor's rotor, in effect the motor's secondary winding, when the latter is short-circuited or closed through an external impedance.[22]The rotating magnetic flux induces currents in the windings of the rotor;[23] in a manner similar to currents induced in a transformer's secondary winding(s). The currents in the rotor windings in turn create magnetic fields in the rotor that react against the stator field. Due to Lenz's Law, the direction of the magnetic field created will be such as to oppose the change in current through the rotor windings. The cause of induced current in the rotor windings is the rotating stator magnetic field, so to oppose the change in rotor-winding currents the rotor will start to rotate in the direction of the rotating stator magnetic field. The rotor accelerates until the

magnitude of induced rotor current and torque balances the applied load. Since rotation at synchronous speed would result in no induced rotor current, an induction motor always operates slower than synchronous speed. The difference, or "slip," between actual and synchronous speed varies from about 0.5 to 5.0% for standard Design B torque curve induction motors.[24] The induction machine's essential character is that it is created solely by induction instead of being separately excited as in synchronous or DC machines or being self-magnetized as in permanent magnet motors.[22]

For rotor currents to be induced, the speed of the physical rotor must be lower than that of the stator's

rotating magnetic field ( ); otherwise the magnetic field would not be moving relative to the rotor conductors and no currents would be induced. As the speed of the rotor drops below synchronous speed, the rotation rate of the magnetic field in the rotor increases, inducing more current in the windings and creating more torque. The ratio between the rotation rate of the magnetic field induced in the rotor and the rotation rate of the stator's rotating field is called slip. Under load, the speed drops and the slip increases enough to create sufficient torque to turn the load. For this reason, induction motors are sometimes referred to as asynchronous motors.[25] An induction motor can be used as an induction generator, or it can be unrolled to form a linear induction motorwhich can directly generate linear motion.

V.DYNAMIC PHASOR CONCEPT

Dynamic phasor (DP) models provide abundant merits, including: 1) the capability of small-signal analysis and 2) availability of large step size simulations. The main idea of DP comes from describing the waveform on interval by Fourier Series [8]:

$$\begin{cases} \langle \frac{dx}{dt} \rangle_k &= \frac{dX_k}{dt} + jk\omega X_k \\ \langle x.y \rangle_k &= \sum_{l=-\infty}^{\infty} (X_{k-l}.Y_l). \end{cases} \quad (3)$$

Equation (3) describes the relationship between the DP of a derivative versus the DP of the original signal while (3) describes the relationship between the DP of a product versus the DPs of the individual variables. In this study, the main aim is to derive the DP model of a distribution system composed of a single-phase PV, a three-phase induction machine, a PFC and distribution lines represented by RL circuits.

The DP models in the frame can be derived by converting the DP model from the positive-, negative-, and zero-sequence reference frame [9]. The original signals in the frame can be expressed by DPs as follows:

$$\begin{bmatrix} x_a \\ x_b \\ x_c \end{bmatrix}(\tau) = \sum_{l=-\infty}^{\infty} e^{jk\omega_s \tau} \underbrace{\frac{1}{\sqrt{3}} \begin{pmatrix} 1 & 1 & 1 \\ \alpha^* & \alpha & 1 \\ \alpha & \alpha^* & 1 \end{pmatrix}}_{M} \begin{bmatrix} X_{p,l} \\ X_{n,l} \\ X_{z,l} \end{bmatrix} \quad (4)$$

where stands for the harmonic component index, is the transformation matrix from to , and , , and stand for positive-, negative-, and zero-sequences. It is easy to see that the DPs of variables have the following relationship with the DPs of -sequences:

$$\begin{bmatrix} X_{a,l} \\ X_{b,l} \\ X_{c,l} \end{bmatrix} = M \begin{bmatrix} X_{p,l} \\ X_{n,l} \\ X_{z,l} \end{bmatrix}. \quad (5)$$

In the next section, after introducing the entire system topology, the DP models of each element will be presented one by one, which will be integrated into the overall system model.

V.SYSTEM CONFIGURATION AND MODELING

The parameters presented in [17] and [19] are utilized for the proposed study system shown in Fig. 1. The distributed system consists of a single-phase PV station installed in phase of the system, a 3-phase induction machine, a 3-phase PFC, and a 3-phase load.

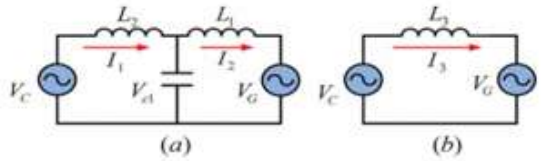

Fig7: Simplified PV model with different filters. (a) LCL filter. (b) L filter.

A. DP Model of a Single-Phase

PV Traditionally, two-stage converters (a DC-AC converter after a DC-DC converter) have been used for PV systems. Two-stage converters need additional devices compared with single-stage converters. Therefore, single-stage converters have been implemented in PV grid integration [20]–[23]. The basic configuration of a single-phase PV is illustrated in

Fig. 2. The main elements of the single-stage PV are the proportional resonant (PR) current controller and the output filters. Fig. 2 shows the basic configuration of an LCL filter in a single-phase PV. It is composed of two inductances and one capacitor connected to the grid through a single-phase transformer. The simplified model of PV connected to the grid with an L or an LCL filter has been illustrated in

Fig. 3. The output voltage of the DC-AC converter is , the filter inductances are and , and the grid side voltage is . Note that the transformer can be represented by an inductor . Therefore, and . Furthermore, for a PV connected to an L filter, if is used for the L filter inductance, . The time-domain equations of the system for the LCL filter are listed as follows:

$$\begin{cases} L_1 \frac{di_1}{dt} & = v_{c1} - v_G \\ L_2 \frac{di_2}{dt} & = v_{con} - v_{c1} \\ C_1 \frac{dv_{c1}}{dt} & = i_2 - i_1. \end{cases} \quad (6)$$

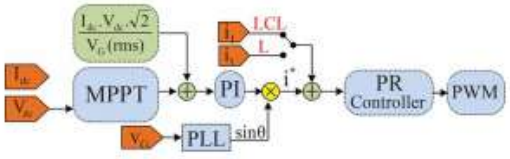

Fig8: Basic control of a single-phase PV.

The dynamics of the PV system with LCL filter in DP is expressed as follows. It should be noted that only the first harmonic is considered for the derivation of dynamic phasor coefficients:

$$\begin{cases} \dot{I}_1 & = \frac{1}{L_1}(V_{c1} - V_G) - j\omega_s I_1 \\ \dot{I}_2 & = \frac{1}{L_2}(V_{con} - V_{c1}) - j\omega_s I_2 \\ \dot{V}_{c1} & = \frac{1}{C_1}(I_2 - I_1) - j\omega_s V_{c1}. \end{cases} \quad (7)$$

It should be noted that is the DP of the output voltage of PV inverter. For an L filter enabled PV system, the basic DP equation of the PV system connected to grid is

$$\dot{I}_3 = \frac{1}{L_3}(V_{con} - V_G) - j\omega_s I_3. \quad (8)$$

A detailed control block diagram of the single-stage single phase PV is illustrated in Fig. 4. It is composed of a maximum power point tracking (MPPT) unit, a proportional resonant (PR) controller, a phase-locked-loop (PLL), and a pulse width modulation (PMW) pulse generation unit. In this paper, the effect of the MPPT dynamics and the PLL has been neglected for simplicity and special attention has been dedicated to the PR controller and the LCL filter.

1) DP Model of a PR Controller:

PR control is used to track ac signals. The PR controller in Fig. 4 tries to provide unity power factor power from the PV. Therefore, the current reference is synchronized with the grid voltage through a PLL. The dynamics of a PR controller considering only the fundamental harmonics can be expressed as

$$\begin{aligned} v_{con} &= (K_p + \frac{K_r s}{s^2 + (\omega_s)^2})(i^* - i_1) \\ &= \left[K_p + K_r(\frac{0.5}{s + j\omega_s} + \frac{0.5}{s - j\omega_s})\right](i^* - i_1) \end{aligned} \quad (9)$$

where is the reference current comes from PV array. In the analytical model, the dynamics of PLL and MPPT are neglected for simplicity of analysis. is the grid current when the PV enhanced with LCL filter. In a case where the PV is interconnected with an L filter, will be replaced by , which is the grid current. The rest of the modeling part has considered the LCL filter only. Define intermediate state variables and , where

$$\begin{cases} (s+j\omega_s)x_1 & = 0.5(i^*-i_1) \\ (s-j\omega_s)x_2 & = 0.5(i^*-i_1). \end{cases} \quad (10)$$

Rewriting (10) in time domain gives (11):

$$\begin{cases} \frac{dx_1}{dt}+j\omega_s x_1 = & 0.5(i^*-i_1) \\ \frac{dx_2}{dt}-j\omega_s x_2 = & 0.5(i^*-i_1). \end{cases} \quad (11)$$

Applying the characteristics of DP, the DP relationship can be derived

$$\begin{cases} \frac{dX_1}{dt} = & 0.5(I^*-I_1)-2j\omega_s X_1 \\ \frac{dX_2}{dt} = & 0.5(I^*-I_1). \end{cases} \quad (12)$$

The DP of the converter output voltage's fundamental frequency component can be expressed as

$$V_{con} = K_{p1}(I^*-I_1)+K_{r1}(X_1+X_2). \quad (13)$$

The DP model of a single-phase PV consists of (7), (12) and (13). The current reference comes from this equation:

$$I^* = \sqrt{2}V_{dc}I_{dc}/V_G(rms) = \sqrt{2}P_{ref}/V_G(rms).$$

B. DP Model of an Induction Machine

Since the single-phase PV will introduce unbalance in the distribution system, the induction machine will be modeled to include unbalance effect. Negative-sequence components in the stator voltage can cause a clockwise rotating stator flux. When this flux is interacting with the counter-clockwise rotating rotor flux, a 120-Hz torque ripple will appear. In turn, the rotating speed will have ripples with 120-Hz frequency. To count in the negative effect, the dynamic model of a three-phase induction machine in [9] based on -sequence components is adopted in this paper. The space-vector model of a squirrel-cage induction machine with magnetic saturation and slot harmonics neglected is presented as follows:

$$\begin{cases} \vec{v}_s = (r_s+L_s\frac{d}{dt})\vec{i}_s+L_m\frac{d}{dt}\vec{i}_r \\ 0 = L_m\frac{d}{dt}\vec{i}_s+(r_r+L_r\frac{d}{dt})\vec{i}_r-j\omega_r\frac{P}{2}(L_m\vec{i}_s+L_r\vec{i}_r) \\ J\frac{d}{dt}\omega_r = \frac{3P}{4}L_m\Im(\vec{i}_s\vec{i}_s^*)-B\omega_r-T_L \end{cases} \quad (14)$$

where denote the stator voltage, stator current, and rotor current, respectively. is the mechanical torque and is the rotor speed. and denote the stator and rotor quantities, respectively. denotes the imaginary part. The DP model of an induction machine can be derived by considering the positiveand negative-sequence components in stator/rotor voltages and currents, as well as the dc and the 120 Hz components in the rotating speed [9].

where subscripts and stand for positive and negative sequence components, respectively.

Since the DP model for the PV system is based on phase , to integrate the induction machine model with the PV system model, the above model will be converted from and to the frame using the relationship presented in (5). The block diagram of the conversion has been illustrated in Fig. 5.

C. PFC and the Integrated System

Considering that there is a three-phase PFC in parallel with the PV, the circuit model of the distribution system can be illustrated as in Fig. 6, where denotes the capacitance of the PFC, is the induction machine's stator current, is the line current, and are the distribution line's parameters, is the load model, and is the system voltage.

For phase , the DP model of the integrated system can be expressed as

$$\begin{cases} \frac{d}{dt}I_p & = \frac{1}{L}(-(j\omega_s L+R)I_p+V_{Gp}-E_p) \\ \frac{d}{dt}V_{Gp} & = \frac{1}{C}\left(-\left(j\omega_s C+\frac{1}{R_L}\right)V_{Gp}-I_{mp}-I_p\right) \end{cases} \quad (17)$$

where represents either phase or phase .

In the proposed system integration approach, individual elements such as PV systems, induction machine loads and resistive loads are modeled as current sources or passive elements. Through the PFC dynamics and the grid inductor dynamics, the individual current sources are then integrated with the grid voltage.

As long as the distribution system is radial, additional unbalanced elements can be modeled as shunt current sources or passive elements and easily

ISSN (Online):2533-8945
VOLUME 3 ISSUE 2

integrated into the overall system model. The entire system is composed of a PV system, an induction machine, a PFC and the RL line. As a total, 17 complex state variables are presented, including the line currents , PFC voltage , induction machine stator currents , induction machine rotor currents , induction machine rotor speed , PV system state variables (output current before filter , voltage across the LCL filter capacitor , and the stator variables in the PR controller of the PV (and). The complex state variables will be separated into real and imaginary components. Therefore, as a total, 34 real state variables are introduced for this DP model and small-signal analysis will show 34 eigenvalues.

VII. SIMULATION RESULTS:

The analytical model for the entire distribution system has been derived in Section III. The model was been built in Matlab/Simulink. The nonlinear analytical model can be linearized based on a certain operating point using Matlab function "linmod". Small-signal analysis can then be carried out for the linearized model. The same study system was also built in Matlab/SimPowerSystems based on the physical circuit connection. The Matlab/SimPowerSystems model captures power electronic switching details and therefore is considered high-fidelity simulation model. Three case studies have been carried out. • In the first case, the analytical model in Simulink is benchmarked with the high-fidelity model in SimPowerSystems.

TABLE I
EIGENVALUES OF THE SYSTEM WITHOUT PV

Eigenvalue	damping ratio %	frequency(Hz)	dominant state
-959 ± 5768i	16.4	918	
-966± 5935i	16.07	945	
-966 ± 5935i	16.06	945	V_G, I
-959 ± 5014i	18.78	798	
-966 ± 5181i	18.33	825	
-966 ± 5181i	18.33	825	
-133.37 ± 308i	39.68	49	I_{ps}
-137.95 ± 117i	76.37	18.6	I_{pr}
-133.38 ± 445i	28.69	70.9	I_{ns}
-137.95 ± 637i	21.15	101	I_{nr}
-0.76 ± 754	0.1	120	ω_{r2}
-1.54 ± 0i	100	0	ω_r

TABLE II
EIGENVALUES OF THE SYSTEM WITH PV

Eigenvalue	damping ratio %	frequency(Hz)	dominant state
-966 ± 5935i	16.06	944	
-967 ± 5848i	16.31	931	
-993 ± 5607i	17.43	892	
-993 ± 4853i	20.04	772	V_G, I
-966 ± 5181i	18.33	824	
-967 ± 5094i	18.65	810	
-855 ± 8475i	10.04	1349	
-855 ± 7721i	11.01	1229	V_{c1}
-1.87 ± 754i	0.25	120	
-1.87 ± 0.10i	99.8	0.02	X_1, X_2
-8218 ± 377i	99.9	60	I_{pv}
-133.37 ± 308i	39.68	49	I_{ps}
-137.96 ± 117i	76.23	18.6	I_{pr}
-133.37 ± 445i	28.68	70.9	I_{ns}
-137.96 ± 637i	21.17	101	I_{nr}
-0.75 ± 754	0.1	120	ω_{r2}
-1.52 ± 0i	100	0	ω_r

Dynamic simulation results are compared for the same dynamic event: a step change in load torque of the induction machine.

• In the second case, the effect of unbalance on the dynamic performance is investigated by applying a ramp change in irradiance of the PV. This dynamic event emulates the cloud effect on a PV and a distribution system.

• In the third case, the effect of the grid-line length on stability is investigated. Small-signal analysis and time-domain simulation are carried out.

A. Case Study 1

In this part, the analytical model-based simulation results are compared with the Matlab/SimPowerSystems model-based simulation results (in short, Simpower). A single-phase PV is connected to the phase of the system at the point of common coupling (PCC) shown as in Fig. 1. At , the induction machine's mechanical torque was applied a step change from 28 N.M to 23 N.M. The simulation results of the electromagnetic torque and the rotor speed of the induction machine have been presented in Fig. 7.

The dynamic responses from the two models match each other well. The simulation results for the line current, the line voltage and the PV current are presented in Fig. 8. The results of the line current and the line voltage from both models match well, which demonstrates the accuracy of the analytical model derived in

ISSN (Online):2533-8945
VOLUME 3 ISSUE 2

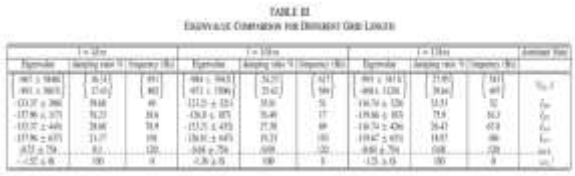

this paper. The PV current from SimPowerSystems simulation has dynamics related to MPPT control and the dc-side capacitor. In the analytical model, MPPT effect and dc-side dynamics are neglected. While the PV power is constant and has negligible variation, therefore the PV current of the analytical model is almost constant.

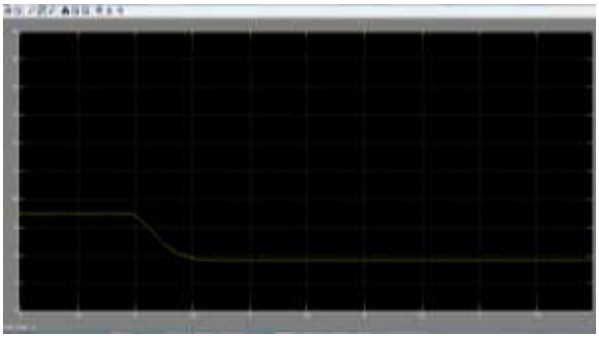

Fig9: Induction machine stator armature current

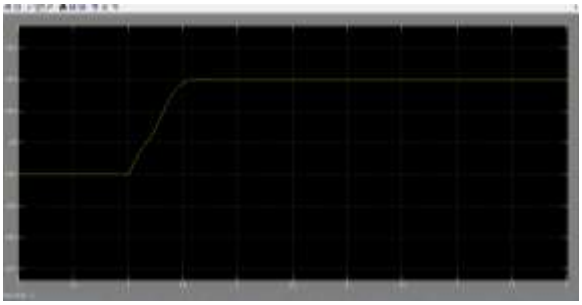

Fig10:Vg RMS

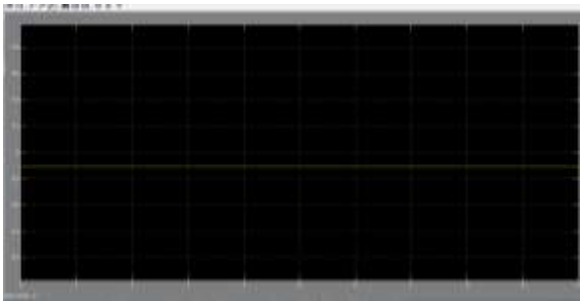

Fig11:Ipv

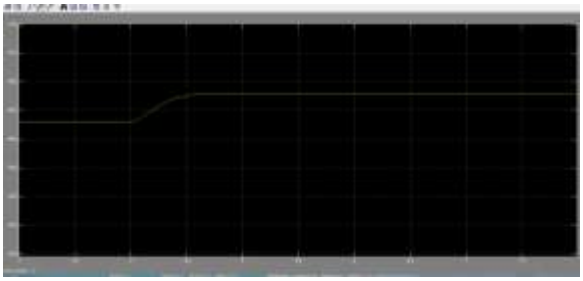

Fig12: Rotor speed

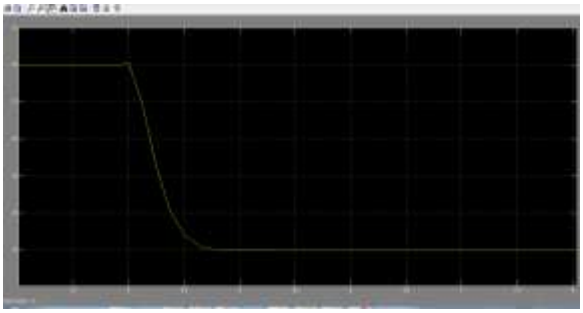

Fig13: Electromagnetic torque

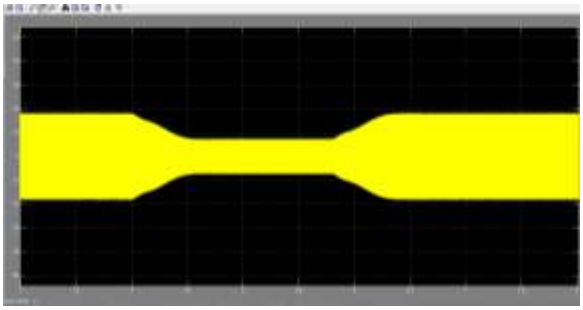

Fig14:Ipv

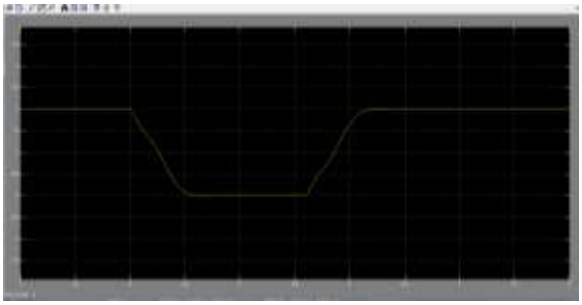

Fig15: Ppv

Fig16: Electromagnetic torque(te)

B. Case Study 2

Eigenvalue analysis for the system with and without PV has been conducted and the results are presented in Tables I and II. It can be observed from the tables that, due to the PV, five pairs of eigenvalues are introduced and these eigenvalues are related to PV state variables such the LCL capacitor voltage , PR controller state variables , , and the PV current . 1) PV Irradiance Change: In this part, the effect of PV irradiance change will be simulated in both Matlab/Simulink and Matlab/SimPowersystems. the PV irradiance was set to previously. A ramp change will be applied at to decrease the irradiance to in 0.2 s. Then after 1.4 s, the irradiance will be set back to . The change of irradiance has been illustrated in detail in the first figure of Fig. 9.

The second figure of Fig. 9 shows the PV power which follows the irradiance command. The PV power of the analytical model is set to follow the change of the irradiance. It is noticed that the maximum power level (2 kW) is obtained when the irradiance is set to . The third figure shows the electrical torque of the induction machine. When the irradiance is decreased due to clouds, the PV power is decreased, which leads to the decrease in the unbalance injection level to the system. The magnitude of the 120-Hz ripple has been decreased during the interval of 4 to 6 s. The last figure shows the PV current which has been decreased due to the irradiance change.

C. Case Study 3

In Case 3, impact of line lengthon system stability was investigated by both eigenvalue analysis and time-domain simulation in Matlab/SimPowerSystems. The eigenvalues of the system are presented in Table III. The movement of the dominant modes is presented in Fig. 10. One of the dominant modes is related to a real-axis eigenvalue. The grid line length has been changed from 3 km to 15 km in order to observe its effect on dynamics. It is worth mentioning that increasing the line length more than 15 km causes non-convergence of the sweeping method for initialization. Therefore the results are only shown for the initial conditions where the system is able to converge.

VII. CONCLUSION

In this paper, a dynamic phasor-based dynamic model was derived for an unbalanced distribution system consisting of

TABLE IV
COMPARISON OF SIMULATION TIME BETWEEN TWO MODELS

Time to be simulated	SimPowerSystems	Simulink
2 sec	4 min and 12 sec	2 sec
4 sec	9 min and 55 sec	4 sec
8 sec	18 min and 33 sec	6 sec
100 sec	Memory error	58 sec

TABLE V
PARAMETERS OF THE INDUCTION MACHINE

Total capacity	5.5 kVA
Nominal voltage	400 V
Frequency	60 Hz
R_s	2.52 Ω
R_r	2.67 Ω
X_{ls}	3.39 Ω
X_{lr}	3.39 Ω
X_M	197 Ω
J	0.486 $kg.m^2$
P (poles)	4

TABLE VI
PARAMETERS OF PV

Total capacity	2000 W
Frequency	60Hz
L_a	0.01 H
L_b	0.02 H
Cap	3 μH
$K_p(PLL)$	180
$K_i(PLL)$	3200
$K_p(PR)$	200
$K_i(PR)$	1500

TABLE VII
LINE DATA OF THE NETWORK

Line No	Line Type	Z (Ω/km)	Length(m)
1	Z_{Grid}	0.579+j1.75	105
2	Z_{IM}	0.497+j2.47	105
3	Z_{PV}	0.462+j0.564	30

a single-phase PV, a three-phase induction machine and a three-phase power factor correction capacitor. The model is capable of fast time-domain simulation and small-signal analysis. The model's accuracy in capturing time-domain dynamics has been validated by Matlab/SimPowerSystems-based simulation. The model's capability of small-signal analysis was also demonstrated. The eigenvalue analysis results corroborate with time-domain simulation results in Matlab/SimPowerSystems.

REFERENCES

[1] M. Braun, G. Arnold, and H. Laukamp, "Plugging into the zeitgeist," IEEE Power Energy Mag., vol. 7, no. 3, pp. 63–76, 2009.

[2] A. K. Abdelsalam, A. M. Massoud, S. Ahmed, and P. N. Enjeti, "Highperformance adaptive perturb and observe MPPT technique for photovoltaic-based microgrids," IEEE Trans. Power Electron., vol. 26, no. 4, pp. 1010–1021, 2011.

[3] H. Kanchev, D. Lu, F. Colas, V. Lazarov, and B. Francois, "Energy management and operational planning of a microgrid with a PV-based active generator for smart grid applications," IEEE Trans. Ind. Electron., vol. 58, no. 10, pp. 4583–4592, 2011.

[4] K. Tan, P. So, Y. Chu, and M. Chen, "Coordinated control and energy management of distributed generation inverters in a microgrid," IEEE Trans. Power Del., vol. 28, no. 2, pp. 704–713, Apr. 2013.

[5] PSCAD Manual, Manitoba HVDC Res. Center [Online]. Available: http://www.pscad.com

[6] SimPowerSystems For Use with Simulink®, TransÉnergie Technologies Hydro-Québec [Online]. Available: http://www.mathworks.com

[7] J. Sun, "Small-signal methods for ac distributed power systems—a review," IEEE Trans. Power Electron., vol. 24, no. 11, pp. 2545–2554, 2009. [8] A. M. Stankovic, B. C. Lesieutre, and T. Aydin, "Modeling and analysis of single-phase induction machines with dynamic phasors," IEEE Trans. Power Syst., vol. 14, no. 1, pp. 9–14, Feb. 1999.

[9] A. M. Stankovic, S. R. Sanders, and T. Aydin, "Dynamic phasors in modeling and analysis of unbalanced polyphase ac machines," IEEE Trans. Energy Convers., vol. 17, no. 1, pp. 107–113, Mar. 2002. [

10] A. M. Stankovic and T. Aydin, "Analysis of asymmetrical faults in power systems using dynamic phasors," IEEE Trans. Power Syst., vol. 15, no. 3, pp. 1062–1068, Aug. 2000.

[11] P. C. Stefanov and A. M. Stankovic, "Modeling of UPFC operation under unbalanced conditions with dynamic phasors," IEEE Trans. Power Syst., vol. 17, no. 2, pp. 395–403, May 2002.

[12] P. Mattavelli, A. M. Stankovic, and G. C. Verghese, "SSR analysis with dynamic phasor model of thyristor-controlled series capacitor," IEEE Trans. Power Syst., vol. 14, no. 1, pp. 200–208, Feb. 1999.

[13] G. Díaz, C. Gonzalez-Moran, J. Gomez-Aleixandre, and A. Diez, "Complex-valued state matrices for simple representation of large autonomous microgrids supplied by and generation," IEEE trans. Power Syst., vol. 24, no. 4, pp. 1720–1730, Nov. 2009.